Cellular/Molecular

Acute Suppression of Spontaneous Neurotransmission Drives Synaptic Potentiation

Elena Nosyreva,[1] Kristen Szabla,[2] Anita E. Autry,[2] Alexey G. Ryazanov,[3] Lisa M. Monteggia,[2] and Ege T. Kavalali[1]

[1]Department of Neuroscience, University of Texas Southwestern Medical Center, Dallas, Texas 75390-9111, [2]Department of Psychiatry, University of Texas Southwestern Medical Center, Dallas, Texas 75390-9111, and [3]The Department of Pharmacology, University of Medicine and Dentistry of New Jersey, Robert Wood Johnson Medical School, Piscataway, New Jersey 08854

The impact of spontaneous neurotransmission on neuronal plasticity remains poorly understood. Here, we show that acute suppression of spontaneous NMDA receptor-mediated (NMDAR-mediated) neurotransmission potentiates synaptic responses in the CA1 regions of rat and mouse hippocampus. This potentiation requires protein synthesis, brain-derived neurotrophic factor expression, eukaryotic elongation factor-2 kinase function, and increased surface expression of AMPA receptors. Our behavioral studies link this same synaptic signaling pathway to the fast-acting antidepressant responses elicited by ketamine. We also show that selective neurotransmitter depletion from spontaneously recycling vesicles triggers synaptic potentiation via the same pathway as NMDAR blockade, demonstrating that presynaptic impairment of spontaneous release, without manipulation of evoked neurotransmission, is sufficient to elicit postsynaptic plasticity. These findings uncover an unexpectedly dynamic impact of spontaneous glutamate release on synaptic efficacy and provide new insight into a key synaptic substrate for rapid antidepressant action.

Introduction

Spontaneous neurotransmitter release, which occurs independent of presynaptic action potentials, is a ubiquitous property of presynaptic nerve terminals (Katz, 1969). Recent work has shown that sustained inhibition of postsynaptic receptors with or without action potential blockade for several hours to days can elicit robust synaptic homeostatic regulation or other forms of synaptic plasticity in several species (Frank et al., 2006; Sutton et al., 2006; Aoto et al., 2008; Lee et al., 2010; Lindskog et al., 2010; Jin et al., 2012). Previous studies have assessed spontaneous unitary synaptic events as a read-out for synaptic efficacy, leaving unanswered whether this form of homeostatic regulation impacts evoked neurotransmission. It is also unclear whether the effects of postsynaptic receptor inhibition are due to suppression of glutamatergic tone mediated by ambient glutamate regardless of vesicular release (Herman and Jahr, 2007; Povysheva and Johnson, 2012), or inhibition of quantal spontaneous excitatory neurotransmission (Sutton et al., 2007).

To date, studies have focused on *in vitro* manipulations to assess the influence of postsynaptic receptor blockade on homeostatic plasticity. However, there has been a growing interest in whether similar mechanisms occur *in vivo*. A particularly intriguing clinical finding is that a single low dose of the NMDA receptor (NMDAR) antagonist ketamine can elicit a rapid antidepressant response with sustained effects lasting for 10–14 d (Berman et al., 2000; Zarate et al., 2006; Price et al., 2009), well beyond the 2–3 h half-life of the drug (Autry et al., 2011). While these data suggest ketamine is mediating its behavioral effects through a synaptic plasticity process, the mechanisms underlying this process remain unknown.

Here, we show that, in agreement with our previous observations (Autry et al., 2011), 30 min suppression of spontaneous NMDAR-mediated neurotransmission elicits rapid potentiation of synaptic responses recorded in the CA1 region of hippocampus, a key brain region involved in antidepressant action (Monteggia et al., 2004). This potentiation requires eEF2 kinase to trigger rapid protein synthesis of BDNF and increases surface expression of AMPA receptors (AMPARs) containing GluA1 and GluA2 subunits. Our behavioral studies link the same synaptic signaling pathway to the fast-acting antidepressant responses elicited by the NMDAR blocker ketamine. The same synaptic potentiation could be elicited by application of a vacuolar ATPase blocker at rest to deplete neurotransmitter selectively from spontaneously recycling vesicles. These findings demonstrate that selective presynaptic impairment of spontaneous release, without alterations in evoked neurotransmission, is sufficient to elicit synaptic potentiation, thus identifying an active role for spontaneous glutamate release in the maintenance of synaptic efficacy.

Materials and Methods

Extracellular field potential recordings

Hippocampal slices (400 μm) were prepared from 20–60-d-old animals (Sprague Dawley rats, eEF2K and BDNF knock-out mice were used as indicated). Animals were anesthetized with isoflurane and decapitated

Received Oct. 25, 2012; revised March 1, 2013; accepted March 11, 2013.

Author contributions: E.N., K.S., A.E.A., L.M.M., and E.T.K. designed research; E.N., K.S., and A.E.A. performed research; A.G.R. contributed unpublished reagents/analytic tools; E.N., K.S., A.E.A., L.M.M., and E.T.K. analyzed data; E.N., K.S., L.M.M., and E.T.K. wrote the paper.

This work was supported by National Institutes of Health Grants MH070727 (L.M.M.) and MH066198 (E.T.K.), as well as funding from the Brain & Behavior Research Foundation (L.M.M. and E.T.K.) and the International Mental Health Research Organization (L.M.M.). We thank members of the Monteggia and Kavalali laboratories for discussions and comments on this manuscript.

Correspondence should be addressed to either of the following: Ege T. Kavalali, Department of Neuroscience, University of Texas Southwestern Medical Center, 5323 Harry Hines Blvd, Dallas, TX 75390-9111, E-mail: ege.kavalali@utsouthwestern.edu; or Lisa M. Monteggia, Department of Psychiatry, University of Texas Southwestern Medical Center, 5323 Harry Hines Blvd, Dallas, TX 75390-9070, E-mail: lisa.monteggia@utsouthwestern.edu.

DOI:10.1523/JNEUROSCI.4998-12.2013

 0270-6474/13/336990-13$15.00/0

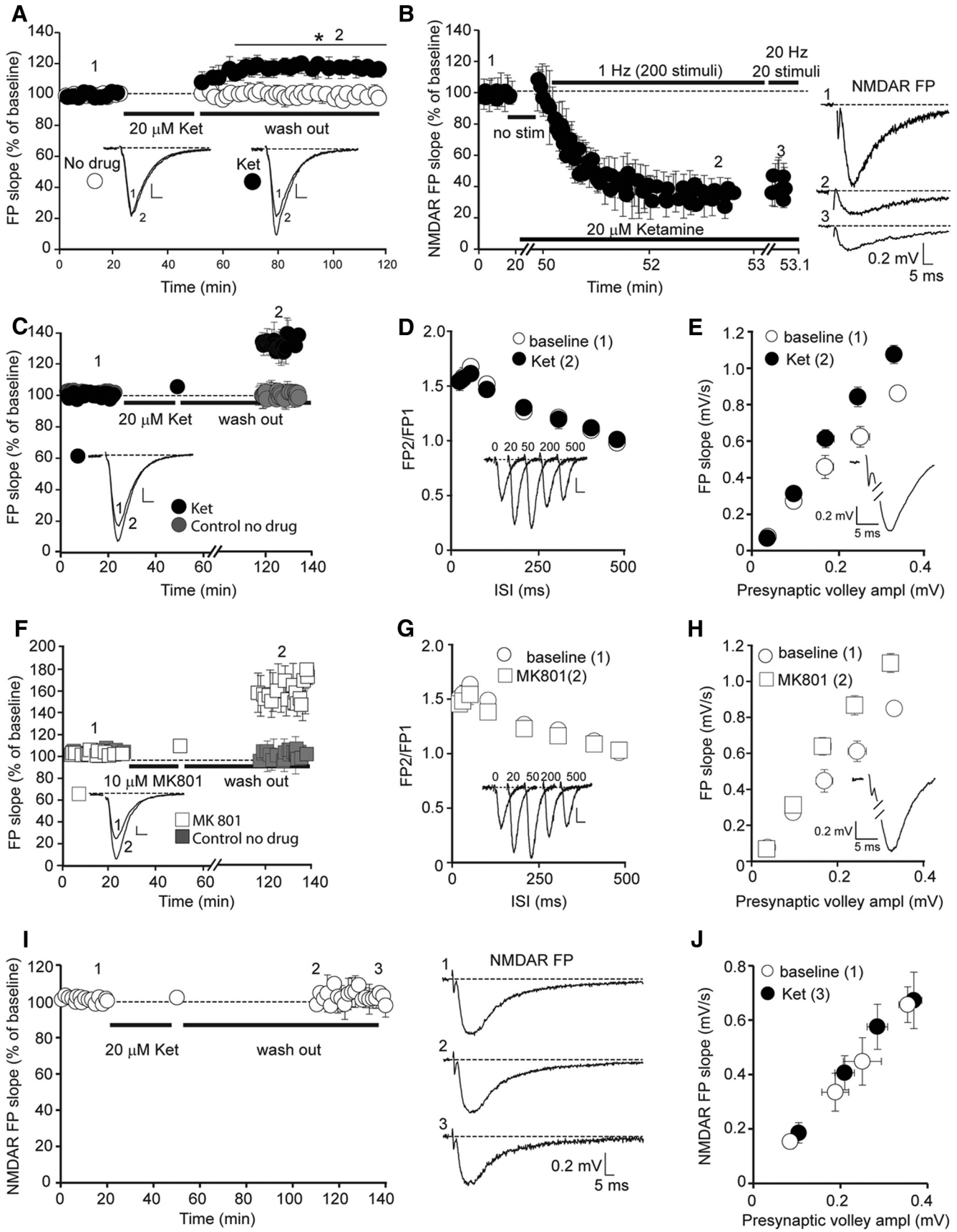

Figure 1. Ketamine application at rest potentiates subsequent AMPAR-mediated evoked neurotransmission. ***A***, FPs were recorded in control ($n = 6$) and ketamine-treated (20 μM) ($n = 12$) slices. Initial FP slopes are plotted as a function of time (mean ± SEM). Inset, Representative waveforms from control and ketamine-treated slices recorded at different time points (1, 2). The line with the asterisk indicates the area of significant change. One-way ANOVA with repeated measurements, $F_{(121,853)} = 2.4$, $p = 0.001$; with Holm-Sidak *post hoc* test, (*Figure legend continues.*)

soon after the disappearance of corneal reflexes. The brain was removed, dissected, and then sliced using a vibratome (VT 1000S, Leica) in ice-cold dissection buffer containing the following (in mM): 2.6 KCl, 1.25 NaH_2PO_4, 26 $NaHCO_3$, 0.5 $CaCl_2$, 5 $MgCl_2$, 212 sucrose, and 10 dextrose. Area CA3 was surgically removed from each slice immediately after sectioning. The slices were transferred into a reservoir chamber filled with ACSF containing the following (in mM): 124 NaCl, 5 KCl, 1.25 NaH_2PO_4, 26 $NaHCO_3$, 2 $CaCl_2$, 2 $MgCl_2$, and 10 dextrose. Slices were allowed to recover for 2–3 h at 30°C. ACSF and dissection buffer were equilibrated with 95% O_2 and 5% CO_2.

For recording, slices were transferred to a submerged recording chamber, maintained at 30°C, and perfused continuously with ACSF at a rate of 2–3 ml/min. NMDAR field potentials were recorded in solution containing the following: 124 mM NaCl, 2 mM KCl, 3 mM $CaCl_2$, 0.1 mM $MgCl_2$, 10 mM glucose, 1.2 mM NaH_2PO_4, 26 mM $NaHCO_3$, 10 μM glycine, 20 μM DNQX (6,7-dinitroquinoxaline-2,3-dione), 50 μM picrotoxin.

Field potentials (FPs) were recorded with extracellular recording electrodes (1 MΩ) filled with ACSF and placed in stratum radiatum of area CA1. FPs were evoked by monophasic stimulation (duration, 200 μs) of Schaffer collateral/commissural afferents with a concentric bipolar tungsten stimulating electrode (Frederick Haer).

Paired-pulse facilitation FPs were elicited by paired-pulse stimulation in slices with interstimulus intervals (ISIs) of 20, 30, 50, 100, 200, 300, 400, and 500 ms, during the baseline and after drug washout. FP2/FP1 ratios (mean ± SEM) were plotted as a function of ISI.

Stable baseline responses were collected every 30 s using a stimulation intensity (10–30 μA), yielding 50–60% of the maximal response. FPs were filtered at 2 kHz and digitized at 10 kHz on a personal computer using custom software (LabVIEW, National Instruments). Synaptic strength was measured as the initial slope (10–40% of the rising phase) of the FP. The group data were analyzed as follows: (1) the initial slopes of the FP were expressed as percentages of the preconditioning baseline average; and (2) the time-matched, normalized data were averaged across experiments and expressed as means ± SEM. For statistical analysis, we used one-way ANOVA with repeated measurements, with Holm-Sidak or Tukey's *post hoc* tests when appropriate. Independent or paired *t* tests were used for statistical analysis, as indicated. In all figures, group data are presented as mean ± SEM.

Whole-cell patch-clamp recordings

Whole-cell recordings were performed on cultured hippocampal pyramidal neurons. Data were acquired using a MultiClamp 700B amplifier and Clampex 9.0 software (Molecular Devices). Recordings were filtered at 2 kHz and sampled at 200 μs. A modified Tyrode's solution was used as external bath solution. This contained the following (in mM): 150 NaCl, 4 KCl, 2 $MgCl_2$, 2 $CaCl_2$, 10 glucose, 10 HEPES, pH 7.4. For isolation of mEPSCs, 1 μM TTX, 50 μM picrotoxin (PTX), and 50 μM AP5 were added. Evoked EPSCs were recorded in presence of 50 μM PTX and 50 μM AP5. The pipette internal solution contained the following (in mM): 115 Cs-$MeSO_3$, 10 CsCl, 5 NaCl, 10 HEPES, 0.6 EGTA, 20 tetraethylammonium-Cl, 4 Mg-ATP, 0.3 Na_3GTP, pH 7.35, and 10 QX-314 [*N*-(2,6-dimethylphenylcarbamoylmethyl)-triethylammonium bromide], 300 mOsm. Field stimulation was applied through concentric bipolar electrodes (FHC) immersed in the perfusion chamber, delivering 15–20 mA pulses. Series resistance values ranged between 10 and 30 MΩ and were left uncompensated (voltage errors, <10 mV).

Behavioral analysis of rapid antidepressant action

Forced swim test. Mice were placed in a 4000 ml Pyrex glass beaker containing 3000 ml of water at 24 ± 1°C for 6 min. Water was changed between subjects. All test sessions were recorded by a video camera positioned on the side of the beakers. The videotapes were analyzed and scored by an observer blind to group assignment during the last 4 min of the 6 min trial.

Novelty suppressed feeding. Briefly, group housed animals were food deprived for 24 h and then placed in a temporary home cage for 30 min. For the test, individual mice were placed in a 42 × 42 cm open-field arena at 40 lux. A single pellet of the mouse's regular food chow was placed in the center of the open-field arena. Each animal was placed in a corner of the arena and allowed to explore for up to 10 min. The trial ended when the mouse chewed a part of the chow. The amount of food consumed in the home cage was taken as weight of chow consumed in 5 min as a control measure for appetite.

Locomotor activity. Mice were placed in cages and locomotor activity was recorded for 2 h under red light by photocell beams linked to computer acquisition software (San Diego Instruments).

Open-field test. Mice were assessed for activity in a 72 × 72 cm open-field arena at 40 lux for 5 min. Movement was tracked by video (EthoVision 3, Noldus) for time spent in center (14 × 14 cm) and peripheral zones (5 cm around perimeter).

Elevated plus maze. Mice were placed in the center of a plus maze (each arm 33 × 5 cm) elevated 1 m above the floor with two open arms and two closed arms (25-cm-tall walls on the closed arms) at 40 lux. The exploratory activity was monitored for 5 min with a video tracking system, and the duration in seconds in the closed and open arms was recorded by EthoVision software.

Dark/light test. Dark/light test was conducted in a two-chambered apparatus with one dark side and one brightly lit side (25 × 26 cm each). Mice were habituated in the dark chamber (2 min) and then the partition between the compartments was removed and mice were allowed to freely explore both chambers (10 min). Movements in the light and the dark chamber were recorded by photocell beams linked to acquisition software (Med Associates).

←

(*Figure legend continued.*) $p < 0.05$. Scale bar, 0.2 mV/5 ms. ***B***, Left, NMDAR FPs as a function of time (mean ± SEM). Ketamine was applied after baseline for 30 min at rest, followed with a train of 200 stimuli at 1 Hz, and 20 stimuli at 20 Hz, in the presence of ketamine ($n = 6$). NMDAR FPs were recorded in solution containing the following: 124 mM NaCl, 2 mM KCl, 3 mM $CaCl_2$, 0.1 mM $MgCl_2$, 10 mM glucose, 1.2 mM NaH_2PO_4, 26 mM $NaHCO_3$, 10 μM glycine, 20 μM DNQX, 50 μM picrotoxin. Right, Representative traces of NMDAR FP recorded during baseline (1), at the end of 1 Hz train (2), and during 20 Hz stimulation (3). ***C***, Different protocol of ketamine application (see Materials and Methods). FP initial slopes from control ($n = 5$) and ketamine-treated slices ($n = 9$) are plotted as a function of time (mean ± SEM). Inset, Representative waveforms from ketamine-treated slices at different time points (1, 2). Synaptic strength increases significantly in ketamine-treated slices, compared with control slices. One-way ANOVA with repeated measurements, $F_{(10,65)} = 7.3$, $p = 0.001$; with Holm-Sidak *post hoc* test, $p < 0.05$. Scale bar, 0.2 mV/5 ms. ***D***, Paired-pulse facilitation. Plotted are FP2/FP1 ratios recorded during baseline (1) and after ketamine application (2) as a function of ISI (mean ± SEM). Inset, Representative traces: 0 FP1 followed by FP2 with 20, 50, 200, and 500 ms ISI. No significant changes were observed in these experiments ($n = 9$). Scale bar, 0.2 mV/5 ms. ***E***, Input–output curves measured during baseline (1) and after ketamine washout (2). Plotted are FP initial slopes (mean ± SEM) as a function of presynaptic volley values at 5, 10, 15, 20, and 25 μA stimulation intensity. The slope of the input–output curve after ketamine treatment (2) is significantly different from the slope measured during baseline (1); (*t* test, $p < 0.05$) ($n = 9$). Inset, Representative FP trace. ***F***, Plotted are FP initial slopes (mean ± SEM) from control slices ($n = 5$) and slices treated with 10 μM MK801 ($n = 5$) as a function of time. Inset, Representative waveforms from MK801-treated slices at different time points (1, 2). Synaptic strength increases significantly in MK801-treated slices while no changes are observed in control slices (Control no drug). One-way ANOVA with repeated measurements, $F_{(37,151)} = 2.75$, $p = 0.001$; with Holm-Sidak *post hoc* test, $p < 0.05$. Scale bar, 0.2 mV/5 ms. ***G***, FPs elicited by paired-pulse stimulation with ISI of 20, 30, 50, 100, 200, 300, 400, and 500 ms during the baseline (open circles) and after MK801 washout (open squares). Plotted are FP2/FP1 ratios (± SEM) as a function of interpulse interval. Inset, Representative traces: 0 FP1 followed by FP2 with 20, 50, 200, and 500 ISI. No significant changes were observed in these experiments ($n = 5$). Scale bar, 0.2 mV/5 ms. ***H***, Input–output curves measured during baseline (1) and after MK801 washout (2). Plotted are FP initial slopes as a function of presynaptic volley values (mean ± SEM) at 5, 10, 15, 20, and 25 μA stimulation intensity. The slope of input–output curve after MK801 treatment is significantly different from the slope without MK801 treatment (*t* test, $p = 0.02$; $n = 5$). Inset, Representative FP trace. ***I***, Left, Plotted are NMDAR FP initial slopes before and after ketamine treatment as a function of time (mean ± SEM). After application of ketamine and 1 h washout, no significant changes in synaptic strength were observed. One-way ANOVA with repeated measurements, $F_{(1,60)} = 14.1$, $p = 0.4$ ($n = 5$). Right, Representative traces of NMDAR FP recorded at different time points (1, 2, 3). ***J***, Input–output curves for NMDAR FP measured during baseline (1) and after ketamine washout (3). Plotted are FP initial slopes as a function of presynaptic volley values (mean ± SEM) at 10, 20, 30, and 40 μA stimulation intensity. There is no significant change in the slope of input–output curves before and after ketamine treatment ($p = 0.44$; $n = 5$).

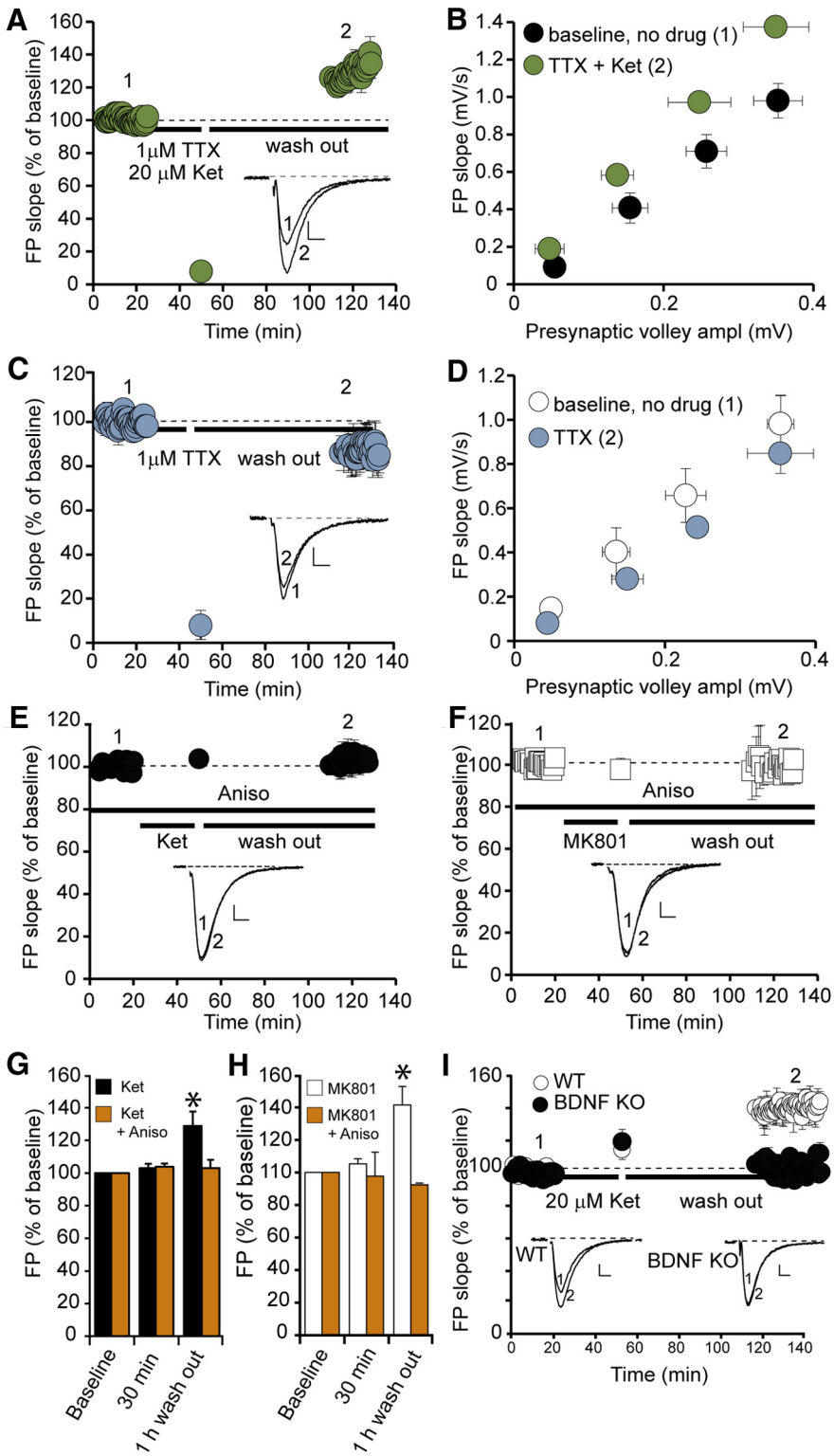

Figure 2. Ketamine-mediated synaptic potentiation occurs in the absence of activity but depends on protein synthesis and BDNF expression. ***A***, Plotted are FP initial slopes after ketamine and TTX treatment as a function of time (mean ± SEM). Inset, Representative waveforms at different time points (1, 2). Synaptic strength increases significantly after treatment with ketamine plus TTX. One-way ANOVA with repeated measurements, $F_{(23,167)} = 6.16$, $p = 0.001$; with Holm-Sidak *post hoc* test, $p < 0.05$; $n = 7$. Scale bar, 0.2 mV/5 ms. ***B***, Input–output curves measured during baseline (1) and after ketamine plus TTX washout (2). Plotted are FP initial slopes as a function of presynaptic volley values at 5, 10, 15, 20, and 25 μA stimulation intensity (mean ± SEM). The slope of input–output curve after ketamine plus TTX treatment is significantly different from the slope measured during baseline (*t* test, $p = 0.01$; $n = 7$). ***C***, Plotted are FP initial slopes after TTX treatment as a function of time (mean ± SEM). Inset, Representative waveforms from TTX-treated slices at different time points (1, 2). There is no significant change in synaptic strength after application of TTX. Scale bar, 0.2 mV/5 ms; $n = 5$. ***D***, Input–output curves measured during baseline (1) and after TTX washout (2). Plotted are FP initial slopes as a function of presynaptic volley values at 5, 10, 15, 20, and 25 μA stimulation intensity (mean ± SEM). There is no significant change in the slope of input–output curve after application of TTX ($n = 5$). ***E***, ***F***, Application of anisomycin (20 μM) for the whole length of the experiment blocks synaptic potentiation induced by ketamine ($n = 9$) or MK801 ($n = 5$). Plotted are FP initial slopes as a function of time (mean ± SEM). Inset, Representative waveforms from ketamine-treated (***E***) and MK801-treated (***F***) slices at different time points (1, 2). ***G***, ***H***, Plotted are average values of FP initial slopes (mean ± SEM) measured during baseline at 30 min of ketamine and MK801 application and after 1 h of washout. Black bars (***G***) and white bars (***H***) are experiments from Fig. 1*C*,*F* (*C*, ketamine; *F*, MK801). Yellow bars, Ketamine or MK801 in presence of anisomycin (Fig. 2*E*,*F*). Scale bar, 0.2 mV/5 ms (***G***, $n = 6$; ***H***, $n = 5$). Both ketamine and MK801 induce significant facilitation in synaptic strength, anisomycin abolishes this effect. ***I***, In wild-type (WT) slices ($n = 5$), ketamine induced synaptic strength facilitation. In contrast, no changes were observed in slices from inducible BDNF knock-out mice after application of ketamine ($n = 9$). Plotted are FP initial slopes as a function of time (mean ± SEM). Inset, Representative waveforms from WT and inducible BDNF knock-out (KO) slices, recorded at different time points (1, 2). Synaptic strength increases significantly in WT ketamine-treated slices but not in slices from the BDNF KO. One-way ANOVA with repeated measurements, $F_{(56,227)} = 2.55$, $p = 0.001$; with Holm-Sidak *post hoc* test, $p < 0.05$. Scale bar, 0.2 mV/5 ms.

Dissociated hippocampal culture

Dissociated hippocampal cultures were prepared as previously described (Kavalali et al., 1999). Briefly, whole hippocampi were dissected from postnatal day 0–3 Sprague Dawley rats. Tissue was trypsinized (10 mg/ml trypsin) for 10 min at 37°C, mechanically dissociated by pipetting, and plated on Matrigel-coated coverslips. Cytosine arabinoside (4 μM AraC, Sigma-Aldrich) was added at day 1 *in vitro* (1 DIV); at 4 DIV, AraC concentration was reduced to 2 μM. All experiments were performed on cultures older than 14 DIV. All experiments were performed on at least three independent cultures.

eEF2 kinase knock-out mice

Heterozygous eEF2 kinase knock-out mice were crossed to obtain eEF2 kinase knock-out and wild-type littermate control mice (Park et al., 2008). Genotype was confirmed by PCR analysis of a DNA sample using the protocol described previously (Park et al., 2008). Adult male mice were age and weight matched (6–12 weeks old) and balanced by genotype for behavioral analysis. Mice were kept on a 12 h light/dark cycle and given access to food and water *ad libitum*. All animal protocols were approved by the Institutional Care and Use Committee at University of Texas Southwestern Medical Center.

BDNF knock-out mice

Inducible BDNF knock-out mice were generated from a trigenic cross of NSE-tTA (neuron-specific enolase promoter-tetracycline transactivator protein), TetOp (tetracycline regulated)-Cre,

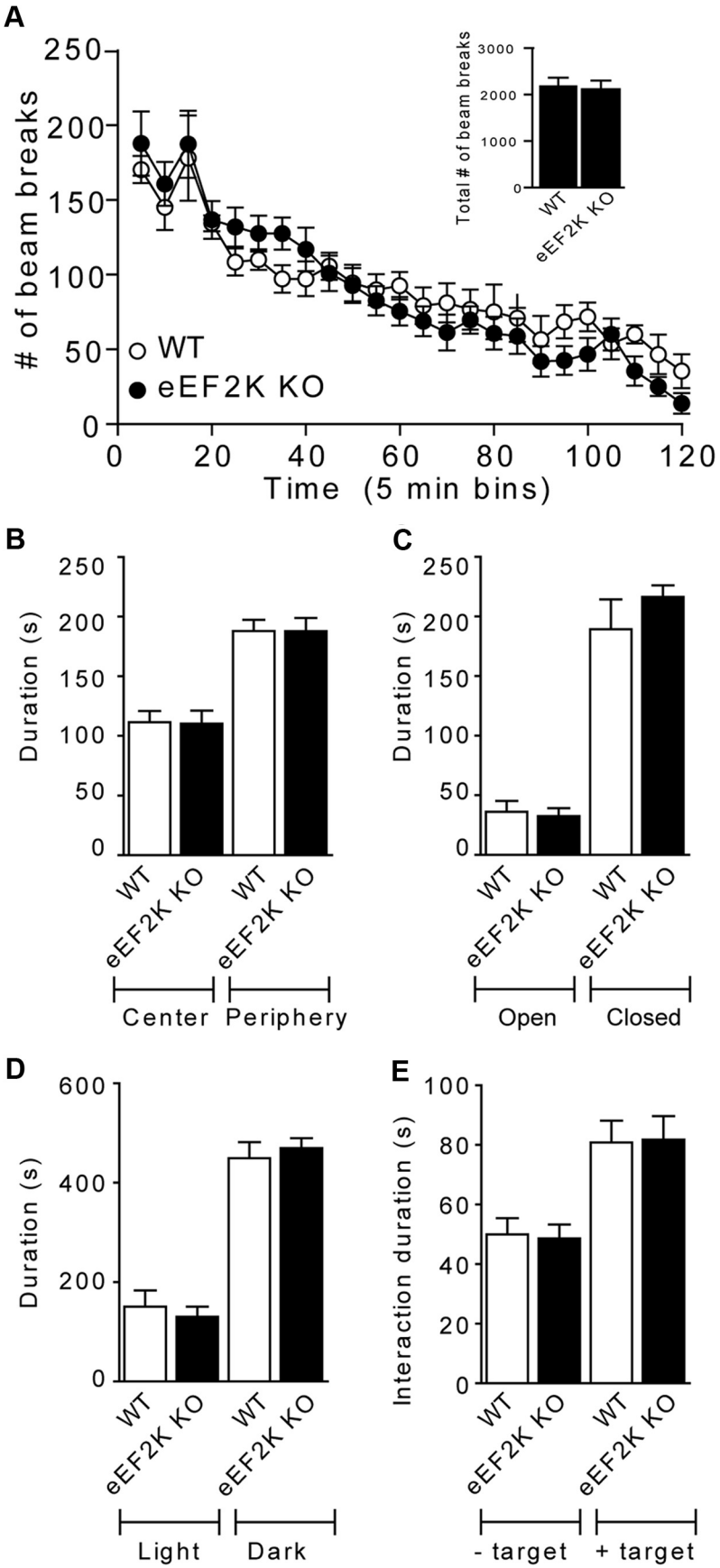

Figure 3. Behavioral characterization reveals no gross phenotypic alterations in adult male mice after loss of eEF2 kinase. ***A***, Analysis of locomotion over a 2 h period reveals no significant difference in locomotor activity between wild-type (WT) littermates and eEF2K knock-outs (KOs) ($n = 8–10$/group) measured either in 5 min increments or in the amount of total activity over a 2 h test period (inset). ***B***, Open-field analysis demonstrates no alterations in anxiety-related behavior between WT littermate controls and eEF2K KOs ($n = 8–10$/group) in time spent in the center or periphery of the arena. ***C***, Elevated plus maze activity shows equivalent behavior between WT littermates and eEF2 kinase KOs ($n = 8–10$/group) in exploration of the closed arm and the open arm. ***D***, Activity in a light/dark chamber shows that WT littermates and eEF2K KOs ($n = 8–10$/group) display comparable movement in each chamber. ***E***, In an interaction chamber, control littermates and eEF2 kinase KOs ($n = 8–10$/group) show no significant differences in time spent with an empty cage or with a social target.

and floxed BDNF mice as previously described (Monteggia et al., 2004).

Western blot analysis

Treatment of hippocampal cultures with ketamine and folimycin. Hippocampal neurons 14–21 DIV were treated with 80 nM folimycin or 20 μM ketamine for 30 min followed by drug washout. One hour after washout of the drugs, samples were collected with 1× loading buffer containing the following (in mM): 62.5 Tris-HCl, pH 6.8, at 25°C, 2% w/v SDS, 10% glycerol, 50 DTT, 0.01% w/v bromophenol blue. Samples were sonicated for 30 s and boiled for 5 min at 95°C. Then 20 μl/well were loaded on SDS on SDS PAGE and analyzed as described below.

Levels of BDNF and phospho-eEF2 proteins in eEF2 kinase knock-out mice. Anterior hippocampal slices (2 per mouse, ~1 mm thick) were dissected from eEF2 kinase knock-out mice or wild-type littermates, which received acute (30 min) saline vehicle or ketamine (5.0 mg/kg) intraperitoneally. Tissue was rapidly frozen on dry ice and lysed in RIPA buffer containing the following: 50 mM Tris, pH 7.4, 1% Igepal, 0.1% SDS, 0.5% Na deoxycholate, 4 mM EDTA, 150 mM NaCl, protease and phosphatase inhibitors (complete minitablets; 10 mM sodium pyrophosphate, 50 mM NaF, 2 mM sodium orthovanadate; Roche). Total protein concentration was quantified by Bradford analysis. Twenty micrograms of total protein per well were loaded on SDS-PAGE gels.

Samples from neuronal cultures, or from hippocampal slices were loaded and separated on 8 or 15% (for BDNF probe) SDS-PAGE gels, then transferred to nitrocellulose membranes.

After blocking for 60 min at room temperature in blocking solution [Tris-buffered saline (TBS), 0.1% Tween 20, 5% w/v nonfat dry milk] blots were washed three times with TBS-T (1× TBS, 0.1% Tween 20) and incubated overnight at 4°C with the following primary antibodies: anti-phospho eEF2 (1:1000), anti-eEF2 (1:1000) (Cell Signaling Technology), anti-BDNF (1:200; Santa Cruz Biotechnology), anti- GAPDH (1:10,000; Cell Signaling Technology) (all rabbit polyclonal antibodies), mouse monoclonal anti-GDP dissociation inhibitor (GDI; 1:15,000) (Synaptic Systems). Primary antibody dilution buffer contained TBS and 0.1% Tween 20 with 5% BSA. After washing three times with TBS-T, blots were incubated with

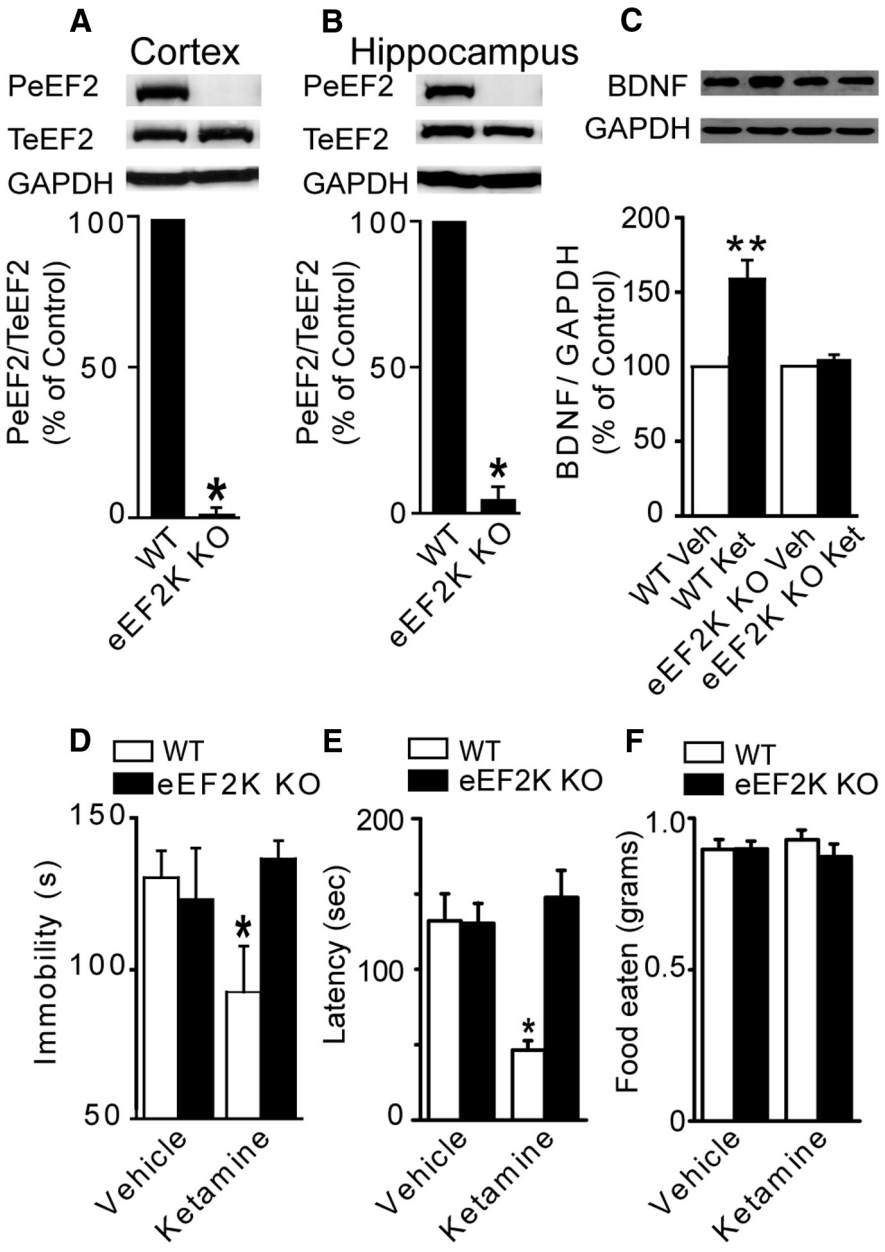

Figure 4. The acute antidepressant-like effects of ketamine requires eEF2 kinase activity. ***A***, ***B***, Immunoblot analysis of phospho-eEF2 and total eEF2 expression in total protein lysates from prefrontal cortex or hippocampus in eEF2 kinase knock-outs (KOs) or wild-type (WT) littermate controls reveals that phosphorylation of eEF2 is negligible after loss of eEF2 kinase (cortex, $p = 0.0054$; hippocampus, $p = 0.0005$) ($n = 5$/group). ***C***, Immunoblot analysis of BDNF expression in WT mice and their eEF2 kinase KO littermates treated for 30 min with vehicle or ketamine (5 mg/kg) illustrates that BDNF expression does not increase in hippocampus after acute ketamine treatment in eEF2 kinase KO mice ($p = 0.138$) ($n = 4$/group). ***D***, Acute ketamine treatment (30 min; 5 mg/kg) decreases immobility in WT animals compared with vehicle-treated mice in the forced swim test. In contrast, their eEF2K KO littermates do not respond to application of ketamine (ANOVA $F_{(1,25)} = 4.530$, Tukey's *post hoc* test, $p < 0.05$; $n = 7–8$ group). ***E***, eEF2 kinase KO mice do not show rapid antidepressant responses to ketamine administration in the novelty suppressed feeding (NSF) paradigm. WT control mice and their eEF2K KO littermates were administered vehicle or ketamine (5.0 mg/kg) intraperitoneally. In NSF test, latency to feed was recorded 30 min after ketamine injection. Ketamine-treated WT control mice show decreased latency to feed (ANOVA, $F_{(3,29)} = 6.487$, $p = 0.0017$ for treatment; with Tukey's *post hoc*, $p < 0.05$); whereas ketamine-treated eEF2K KO animals show no change in latency to acquire food. ***F***, Post-test for the 30 min NSF test demonstrating that all groups show comparable appetites.

HRP-conjugated anti-rabbit (1:2000; Cell Signaling Technology) or anti-mouse (1:5000; Millipore Bioscience Research Reagents) secondary antibodies. Immunoreactive bands were visualized by enhanced chemiluminescence, captured on autoradiography film (Eastman Kodak). Digital images were produced by densitometric scans of autoradiographs and quantified using ImageJ software.

For the samples from neuronal cultures, the amount of total eEF2 protein was normalized to glyceraldehyde 3-phosphate dehydrogenase (GAPDH) loading control. The phospho/total protein ratios were calculated for each condition and presented as a percentage of condition control.

For the samples from mice hippocampi, the amount of BDNF was normalized to GAPDH bands, and phospho-eEF2 and total eEF2 bands were taken as a ratio of GAPDH normalized values.

Drug treatment

DNQX (Sigma-Aldrich), TTX (Calbiochem), PTX (Sigma-Aldrich), ketamine (Fort Dodge Animal Health), folimycin (Sigma-Aldrich), MK801 (Sigma-Aldrich), anisomycin (Sigma-Aldrich), and AP5 (Sigma-Aldrich) were added to solutions as indicated.

When recording FPs, after 20 min of stable baseline, drugs (ketamine, MK801, folimycin, TTX) were applied for 30 min at rest and then one control stimulus was applied, after which there was no stimulation during 1 h washout. Stimulation was resumed for 20 min after washout.

Biochemical measurements of AMPAR surface expression

Cell surface biotinylation experiments were performed as previously described (Chung et al., 2000; Heynen et al., 2003). For these experiments, wild-type and eEF2 kinase knock-out animals were injected intraperitoneally with vehicle or ketamine (5.0 mg/kg). At 3 h, hippocampal slices (1000 μm) were obtained. From each mouse, 2–3 slices were pooled together for one condition. Slices were placed on ice to stop endocytosis, washed with ACSF, and incubated in ACSF containing 0.8 mM sulfo-NHS-LC-biotin (Pierce) for 10 min on ice. The biotin reactions were quenched by incubating slices on ice for 5 min in TBS containing 15 mM ammonium chloride (Sigma-Aldrich) and subsequently washing with ice-cold TBS two times, 5 min each. The slices were then homogenized in a modified RIPA buffer containing 50 mM Tris-HCl, pH 7.4, 1.0% Igepal, 0.1% SDS, 0.5% Na-deoxycholate, 150 mM NaCl, 4 mM EDTA, 50 mM NaH_2PO_4, 50 mM NaF, 10 mM $Na_4P_2O_7$, 1 mM Na_3VO_4, and protease inhibitor mixture (Roche) and solubilized for 1 h at 4°C. Nonsolubilized material was removed by centrifugation (10,000 × *g*) at 4°C for 10 min and supernatant protein concentration was determined using a bicinchoninic acid assay (Pierce). Twenty micrograms of protein from each sample were removed for total protein analysis, and 150 μg of protein from each sample were incubated with 100 μl of washed UltraLink NeutrAvidin (Pierce) immobilized beads for 3 h at 4°C with rotation. Beads were then washed with 10 volumes of RIPA buffer and then eluted with SDS-PAGE sample buffer supplemented with 50 mM dithiothreitol for 20 min at 90°C. Both total and biotinylated proteins were resolved by SDS-

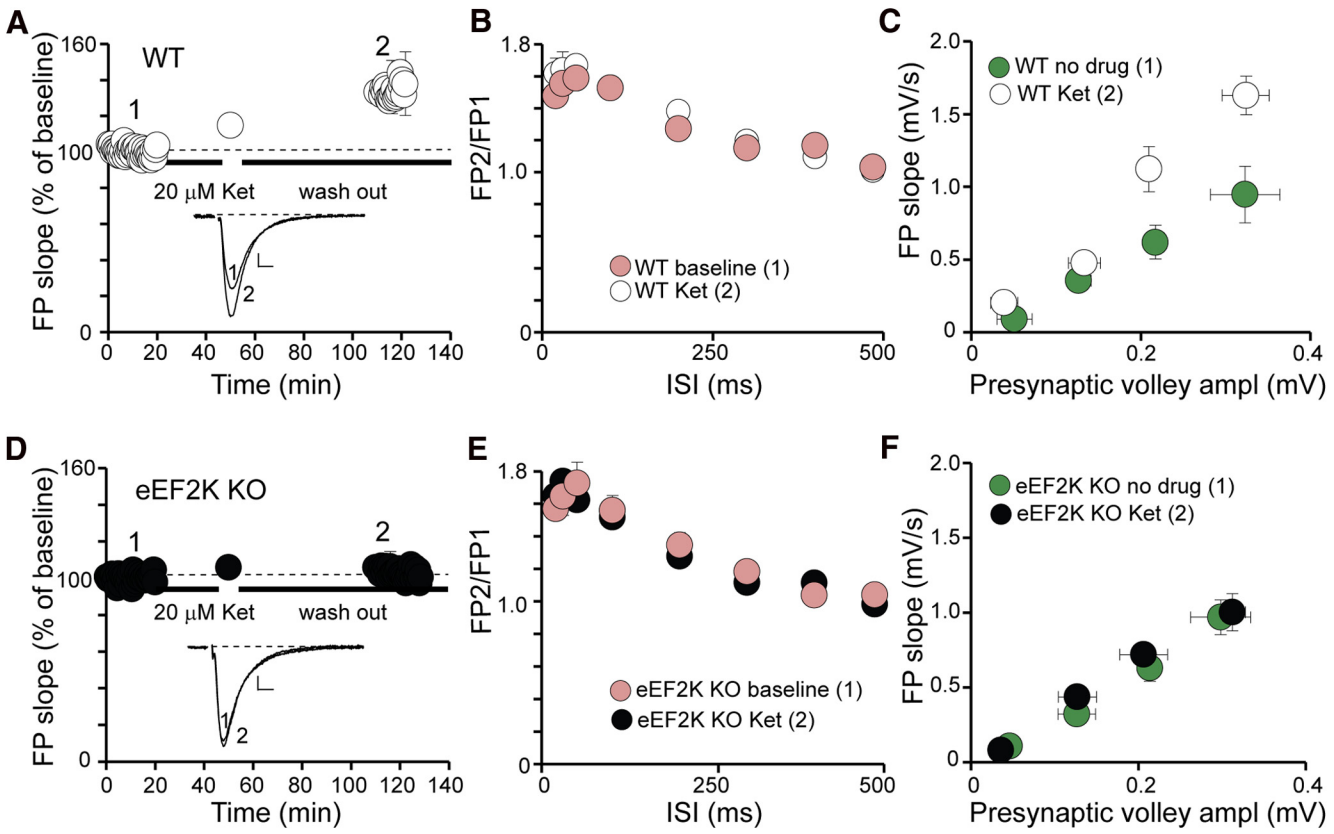

Figure 5. Ketamine-mediated synaptic potentiation requires eEF2 kinase activity. ***A***, ***D***, Plotted are FP initial slopes as a function of time (mean ± SEM) from wild-type (WT) ($n = 6$) and eEF2K knock-out (KO) ($n = 7$) mice slices treated with ketamine. Inset, Representative waveforms from ketamine-treated slices during different time points (1, 2). Synaptic strength increases significantly in ketamine-treated slices from WT mice, but not in eEF2K KO mice. One-way ANOVA with repeated measurements, $F_{(16,101)} = 10.9$, $p = 0.001$; with Holm-Sidak *post hoc* test, $p < 0.05$. Scale bar, 0.2 mV/5 ms. ***B***, ***E***, Paired-pulse facilitation. FPs elicited by paired-pulse stimulation in slices from WT and eEF2K KO mice, during the baseline (1) and after ketamine washout (2). Plotted are FP2/FP1 ratios as a function of ISI (mean ± SEM). No significant changes were observed in these experiments. Scale bar, 0.2 mV/5 ms. ***C***, ***F***, Input–output curves measured in slices from WT and eEF2K KO mice during baseline (1) and after ketamine washout (2). Plotted are FP initial slopes as a function of presynaptic volley values at 5, 10, 15, 20, and 25 μA stimulation intensity (mean ± SEM). The slope of input–output curve after ketamine treatment of WT slices increases significantly (***C***) (*t* test, $p = 0.009$). In the case of eEF2K KO, there is no change in the slope of input–output curve (***F***).

PAGE, transferred to nitrocellulose, and probed with anti-GluA1 N-terminal antibody (1:5000; Millipore Bioscience Research Reagents), anti-GluA2 N-terminal antibody (1:2000; Millipore), and anti-GAPDH antibody (1:50,000; Cell Signaling Technology). Immunoreactive bands were visualized by enhanced chemoluminescence and captured on autoradiography film (Light Labs). Densitometric scans of the autoradiographs were quantified using ImageJ software. The surface/total protein ratios were calculated for each condition. When duplicate conditions were performed within one animal, ratio values were averaged to obtain an animal average for that condition. Therefore, the *n* values for the biotinylation experiments shown in Figure 6 represent the number of mice as opposed to slices. Significant differences between surface/total ratios of treated and control wild-type and eEF2 kinase knock-out slices were determined by a one-way ANOVA combined with Tukey's *post hoc* analysis for multiple comparisons. Although raw ratio values were used for statistical comparisons, the group data are presented in Figure 6 as a percentage of the wild-type control condition to compare across different treatment groups.

Results

NMDAR blockade at rest potentiates subsequent AMPAR-mediated evoked neurotransmission

To elucidate the impact of NMDAR block on synaptic transmission, we examined the efficacy of evoked excitatory synaptic transmission detected at the CA1 region of dissected hippocampal slices exposed to acute ketamine treatment. For this purpose, we stimulated CA3-CA1 Schaffer collateral synapses (1 stimulus per 30 s) and recorded field EPSPs (fEPSPs) at the stratum radiatum elicited by activation of AMPARs. Following an initial baseline period, we stopped stimulation and applied ketamine (20 μM) for 30 min. Once we resumed stimulation (1 stimulus per 30 s), we detected significant potentiation of evoked fEPSPs in hippocampal slices above the initial baseline level, which was sustained for the duration of the 1 h recording following ketamine removal (Fig. 1*A*). The cessation of synaptic stimulation for 30 min alone was not sufficient to trigger this form of synaptic potentiation, suggesting the plasticity was mediated by ketamine (Fig. 1*A*). These observations replicate our findings presented in an earlier study, where we reported an increase in synaptic efficacy after ketamine application at rest (Autry et al., 2011). In parallel experiments, we assessed the impact of ketamine application on pharmacologically isolated fEPSPs mediated by NMDARs (Fig. 1*B*). We observed that ketamine application at rest for 30 min does not alter subsequent evoked NMDAR-mediated transmission. Nevertheless, 1 Hz stimulation in the presence of ketamine causes rapid use-dependent suppression of NMDA fEPSPs (Fig. 1*B*). In this setting, additional 20 Hz stimulation in the presence of ketamine did not suppress NMDA fEPSPs further, suggesting that NMDAR block by ketamine (at 20 μM) reached completion (Fig. 1*B*). We obtained similar findings with application of MK801, a slowly reversible use-dependent NMDAR antagonist, validating the premise that the potentiation was mediated by NMDAR block (data not shown). Although application of these compounds at rest does not appear to alter

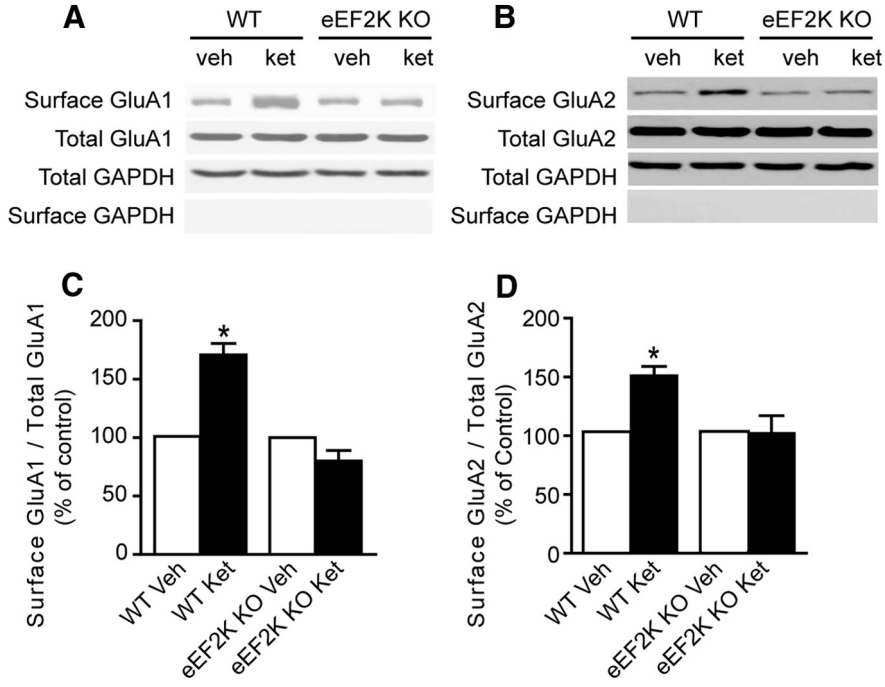

Figure 6. Ketamine-mediated synaptic potentiation requires GluA2 function. Biochemical measurements of surface expressed AMPARs in eEF2K knock-out (KO) mice after application of ketamine. Vehicle or ketamine (5.0 mg/kg) was administered intraperitoneally to wild-type (WT) and eEF2K KO animals. After 3 h, surface levels of GluA1 and GluA2 were assessed using a standard cell surface biotinylation procedure. ***A***, ***C***, Densitometric analysis of surface GluA1/total GluA1 ratios (normalized to control) 3 h after ketamine administration shows that ketamine increases surface GluA1 levels in control animals and has no effect on surface GluA1 levels in eEF2 KO animals (1-way ANOVA, $F_{(3,14)} = 22.50$, $p < 0.0001$ for treatment; Tukey's *post hoc* test, $p < 0.05$; $n = 5–6$/group). ***B***, ***D***, Densitometric analysis of surface GluA2/total GluA2 ratios (normalized to control) 3 h after ketamine administration. Ketamine potentiates surface GluA2 levels in control animals and does not alter surface GluA2 levels in KO animals (1-way ANOVA, $F_{(3,14)} = 5.863$, $p = 0.0121$; Tukey's *post hoc* test, $p < 0.05$; $n = 5–6$/group).

subsequent evoked NMDAR-mediated transmission, we have previously demonstrated that a 30 min application of either ketamine or MK801 in the absence of activity is sufficient to suppress NMDAR-mediated miniature spontaneous neurotransmission (Atasoy et al., 2008; Autry et al., 2011). However, it is important to note that the inhibition of NMDA mEPSCs by ketamine or MK-801 is expected to be less effective in the presence of physiological concentrations of Mg^{2+} (Kotermanski and Johnson, 2009). Collectively, these findings are consistent with the premise that use-dependent NMDAR blockers solely act on a specific mode of neurotransmission that occurs during drug application. This specificity is consistent with the earlier result that the receptors activated at rest or during evoked neurotransmission do not show significant overlap (Atasoy et al., 2008).

We next examined whether the fEPSP potentiation detected after drug elimination was affected by the very low-frequency stimulation (0.033 Hz) applied to test synaptic efficacy during drug removal. To eliminate the potential role of test stimulation and to allow sufficient time for drug removal, ketamine or MK801 were applied for 30 min in the absence of stimulation and slices were subsequently perfused with drug-free ACSF without any extrinsic stimulation for an additional 1 h (Fig. 1*C*,*F*). When we subsequently probed evoked fEPSPs, we detected significant potentiation of synaptic responses above the baseline levels. Repeating the same experimental protocol without ketamine or MK801 application did not elicit synaptic potentiation, indicating that the effect was mediated by NMDAR blockade (Fig. 1*C*,*F*, gray symbols). Under these conditions, treatment with ketamine or MK801 did not alter paired-pulse ratios (Fig. 1*D*,*G*), but caused an increase in the slope of input–output curves, suggesting an increase in the number of synapses activated in response to single stimuli or an increase in the responsiveness of individual postsynaptic sites to glutamate release rather than an increase in neurotransmitter release probability (Fig. 1*E*,*H*).

To investigate whether the potentiation of synaptic efficacy seen after ketamine application involves an increase in the number of active synapses, we monitored the impact of ketamine perfusion at rest on subsequent NMDA fEPSPs (Fig. 1*I*). Under these conditions, a 30 min perfusion of ketamine did not elicit a significant increase in NMDA fEPSPs recorded 1 h after drug removal (Fig. 1*I*). Moreover, in contrast to its augmentation of AMPA fEPSPs, ketamine application did not alter the slope of NMDA-fEPSP input–output curves (Fig. 1*J*). These results indicate that ketamine application does not increase the number of synaptic inputs or modify subsequent NMDAR-mediated responses, but selectively augments AMPAR-mediated neurotransmission within 1 h.

Ketamine-mediated synaptic potentiation occurs in the absence of activity but depends on protein synthesis and BDNF expression

In these experiments, we attempted to minimize the impact of background activity by removing the CA3 cell body layer before recordings. However, this manipulation cannot exclude some residual asynchronous action potential activity that cannot be detected by field electrodes and could possibly contribute to the synaptic potentiation observed after ketamine removal. To assess the potential role of this background activity, slices were perfused with a mixture of ketamine and TTX to block background action potential firing (Fig. 2*A*,*C*). This treatment fully suppressed evoked neurotransmission during drug perfusion but did not prevent synaptic potentiation seen 1 h after drug removal (Fig. 2*A*) or the significant increase in the slope of input–output curves (Fig. 2*B*). Under identical conditions, application of TTX alone did not elicit detectable potentiation or a significant change in input–output relationships seen after drug removal. However, a trend for synaptic depression and a decrease in the slope of the input–output curves was observed, presumably due to the presence of residual TTX, which did not reach significance (Fig. 2*C*,*D*). This result supports a key role for spontaneous glutamate release-driven NMDAR-dependent miniature events in the maintenance of synaptic efficacy. This premise is consistent with our previous analysis, which found that ~20% of total charge carried by spontaneous miniature EPSCs (mEPSCs) is transferred by NMDARs under physiological conditions (Espinosa and Kavalali, 2009).

Previous work has demonstrated that the fast-acting antidepressant effects of ketamine in mouse models are protein synthesis-dependent and require rapid synthesis of BDNF (Autry et al., 2011). To explore the parallels between this particular form of synaptic potentiation observed after ketamine or MK801 application and the antidepressant effects of ketamine, we examined the requirement for rapid protein synthesis in the former.

Hippocampal slices perfused with the protein synthesis inhibitor anisomycin (20 μM), after 20 min of stable baseline recording, did not display significant change in synaptic transmission (1-way ANOVA with repeated measurements, $F_{(1,125)} = 11.45$, $p = 0.195$, $n = 5$; Huber et al., 2000). However, under the same conditions, treatment with ketamine (Fig. 2*E*,*G*) or MK801 (Fig. 2*F*,*H*) did not elicit a significant potentiation of synaptic responses, indicating that the potentiation was dependent on new protein synthesis. We next evaluated whether the synaptic potentiation observed after ketamine application at rest required BDNF expression. In agreement with our earlier findings, hippocampal slices obtained from wild-type littermate control mice showed robust potentiation following ketamine washout (Fig. 2*I*). In contrast, while ketamine treatment of hippocampal slices from brain-specific inducible BDNF knock-outs resulted in a slight initial augmentation, there was no sustained potentiation seen after 1 h drug removal as levels returned to baseline (Fig. 2*I*). The initial residual potentiation observed following ketamine administration in the inducible knock-outs may reflect the low level of BDNF expression still present in these mice (Monteggia et al., 2004).

Ketamine-mediated synaptic potentiation requires eEF2 kinase activity and GluA2 function

To investigate the signal transduction mechanism that links suppression of NMDAR activity at rest to the increase in protein translation and subsequent potentiation of synaptic efficacy, we examined the role of eukaryotic elongation factor 2 (eEF2) kinase. Previous work using hippocampal neuronal cultures found that resting NMDAR-mediated neurotransmission suppresses local dendritic protein translation via activation of eEF2 kinase, keeping eEF2 in a phosphorylated state and thus inhibiting protein translation (Sutton et al., 2007). In agreement with these *in vitro* findings, we previously demonstrated that a single acute injection of ketamine, which triggers a fast-acting antidepressant response, blocks NMDARs at rest and deactivates eEF2 kinase, resulting in a reduction of eEF2 phosphorylation and desuppression of BDNF translation (Autry et al., 2011). To test the applicability of this premise in the context of the augmented synaptic potentiation responses observed following ketamine treatment, we used constitutive eEF2 kinase knock-out mice (Ryazanov, 2002; Park et al., 2008). Behavioral characterization of constitutive eEF2 kinase knock-out

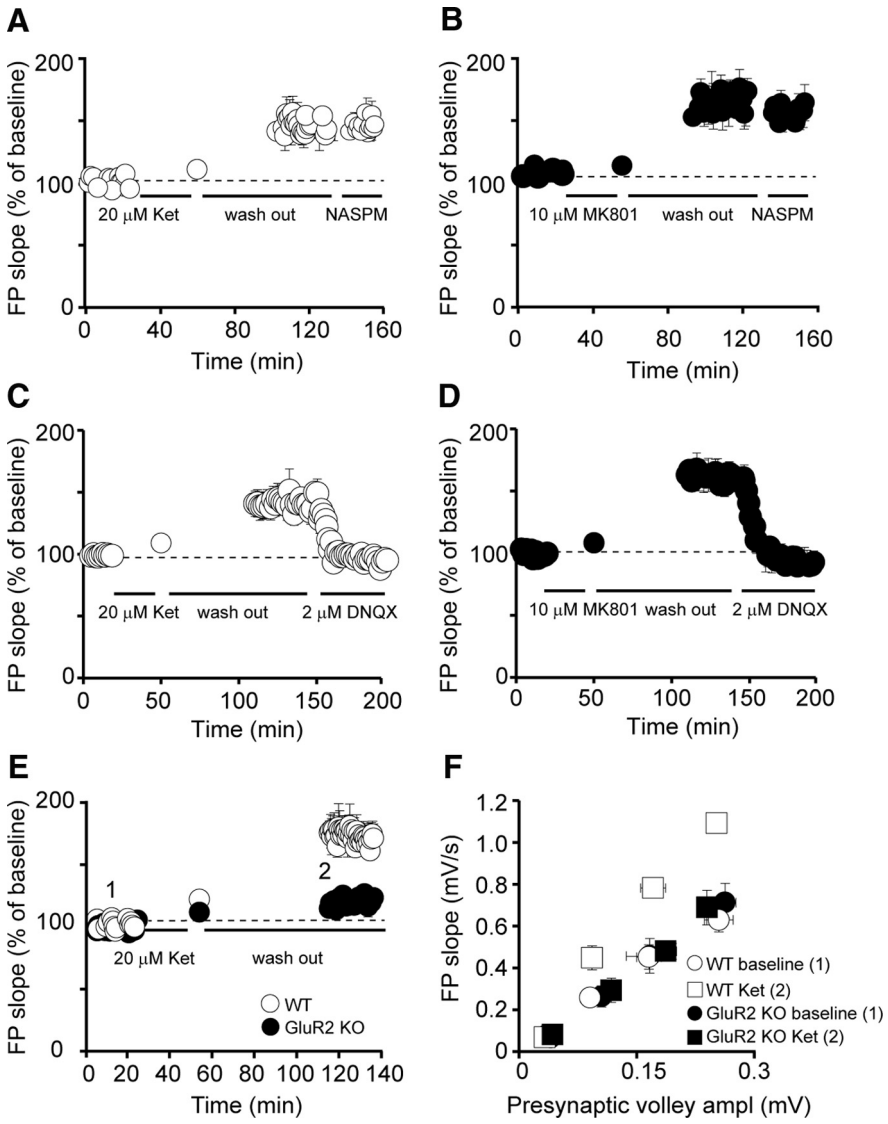

Figure 7. Ketamine-mediated synaptic potentiation requires GluA2 function. ***A***, ***B***, Application of NASPM does not reverse the effect of MK801 and ketamine on synaptic strength. After 20 min of stable baseline the drug was applied [***A***, ketamine (20 μM); ***B***, MK801 (10 μM)] for 30 min at rest, then one control stimulus was applied, after which there was no stimulation during 1 h washout. Stimulation was resumed for 20 min after washout (ketamine, $n = 5$; MK801, $n = 5$). Application of NASPM (10 μM) followed. Plotted are FP initial slopes (mean ± SEM) as a function of time. ***A***, Ketamine induced significant increase in synaptic strength (1-way ANOVA with repeated measurements, $F_{(79,399)} = 34.038$, $p = 0.001$; with Holm-Sidak *post hoc* test, $p < 0.05$). Application of NASPM did not induce a decrease in synaptic strength. ***B***, MK801 induced significant increase in synaptic strength (1-way ANOVA with repeated measurements, $F_{(79,399)} = 22.491$, $p = 0.001$; with Holm-Sidak *post hoc* test, $p < 0.05$). Application of NASPM did not induce a decrease in synaptic strength. ***C***, ***D***, Application of DNQX in low concentration reverses the effect of ketamine and MK801. Ketamine and MK801 were applied as in ***A*** and ***B***. Plotted are FP initial slopes (mean ± SEM) as a function of time. ***C***, Ketamine induced significant increase in synaptic strength (1-way ANOVA with repeated measurements, $F_{(1,247)} = 730$, $p < 0.005$; with Holm-Sidak *post hoc* test, $p < 0.05$. Application of low-dose (2 μM) DNQX reduced the synaptic potentiation seen after ketamine application ($n = 5$). ***D***, MK801 induced significant increase in synaptic strength (1-way ANOVA with repeated measurements, $F_{(1,314)} = 3856$, $p < 0.001$; with Holm-Sidak *post hoc* test, $p < 0.05$). Application of low-dose (2 μM) DNQX could again inhibit the synaptic potentiation seen after MK801 application ($n = 5$). ***E***, Ketamine (20 μM) was applied to hippocampal slices from GluA2 knock-out (KO) mice and their wild-type (WT) littermates (WT, $n = 5$; GluA2 KO, $n = 6$). Plotted are FP initial slopes (mean ± SEM) as a function of time. Ketamine did not induce significant change in synaptic strength in slices from GluA2 KO mice, although in slices from WT littermates, significant increases in synaptic strength were observed after treatment with ketamine (1-way ANOVA with repeated measurements, $F_{(1,319)} = 20.21$, $p < 0,01$; with Holm-Sidak *post hoc* test, $p < 0.05$). ***F***, Input–output curves measured in slices from WT mice ($n = 5$) (open circles and squares) and from GluA2 KO mice (black circles and squares) at different time points (1, 2). The slope of input–output curve after ketamine treatment of WT slices is significantly different from the slope before ketamine treatment ($n = 5$, $p < 0.05$), but there is no significant change in input–output curve slope in slices from GluA2 KO animals ($n = 6$).

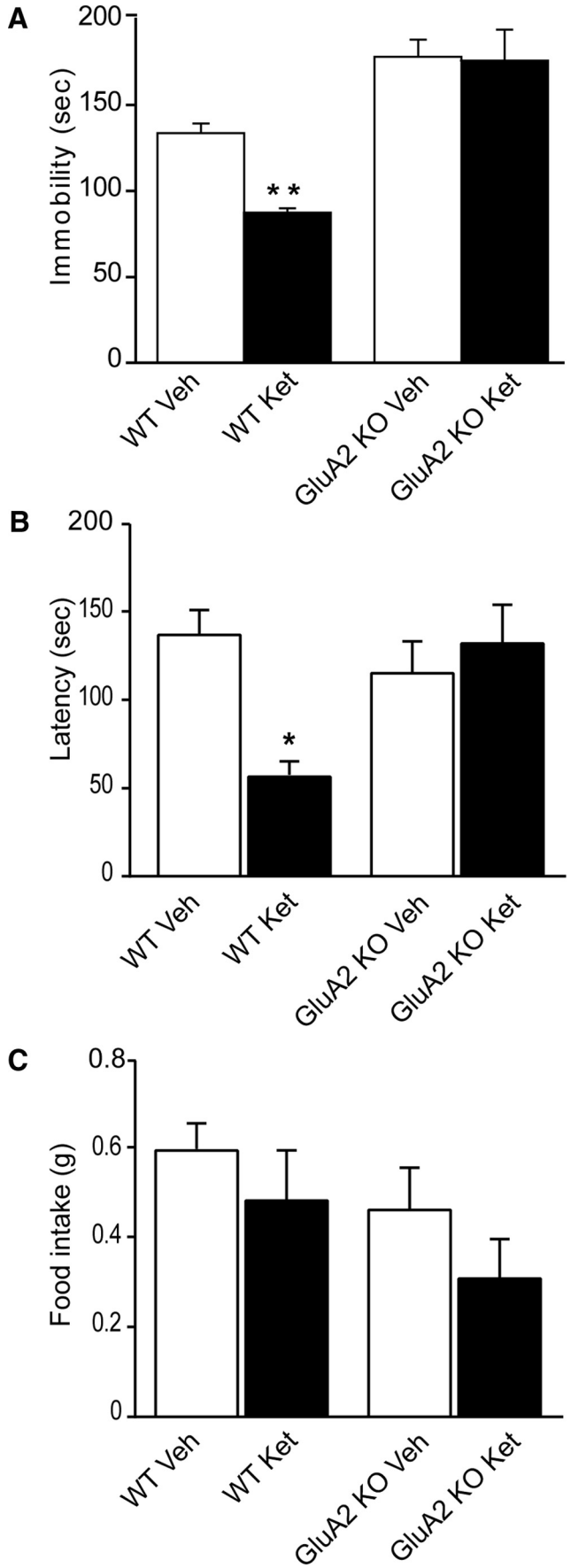

Figure 8. The acute antidepressant-like effects of ketamine is not manifested in GluA2 knock-out (KO) mice. ***A***, The acute antidepressant-like effects of ketamine were examined at 30 min after intraperitoneal injection of either vehicle or ketamine (5.0 mg/kg) in wild-type (WT) and GluA2 KO mice using the forced swim test. Immobility in forced swim test is presented. Ketamine induces significantly less immobility in WT mice (ANOVA, $F_{(3,19)} = 18.88$, $p < 0.0001$; Tukey's *post hoc*, $p < 0.005$; $n = 9–10$/group). Ketamine does not alter immobility in the GluA2 KO mice. ***B***, ***C***, WT and GluA2 KO animals were administered ketamine (5.0 mg/kg) or vehicle intraperitoneally. ***B***, In novelty suppressed feeding (NSF) test 30 min after drug application, ketamine-treated WT mice show significantly decreased latency to feed (ANOVA, $F_{(3,23)} = 3.439$, $p = 0.0365$; with Tukey's *post hoc* test, $p < 0.05$), whereas ketamine-treated GluA2 KO animals show no change in latency to acquire food. ***C***, Post-test for the 30 min NSF test demonstrating that all groups show comparable appetite.

mice did not reveal any alterations in locomotor activity, anxiety-like behavior, or social interaction compared with wild-type littermate controls (Fig. 3). Western blot analysis revealed a negligible level of eEF2 phosphorylation within cortex as well as hippocampus (Fig. 4*A*,*B*). A single low-dose ketamine treatment that triggers an antidepressant response in mice failed to increase BDNF protein levels in the hippocampus of eEF2 kinase knock-out mice (Fig. 4*C*) and did not trigger an antidepressant response in the eEF2 kinase knock-out mice in the forced swim test (Fig. 4*D*) or the novelty-suppressed feeding paradigm (Fig. 4*E*,*F*). These data provide additional support that ketamine's fast-acting antidepressant response requires eEF2 kinase (Fig. 4*D–F*). Following this behavioral validation, we examined whether ketamine application in hippocampal slices from the eEF2 kinase knock-out mice impacted synaptic potentiation. Consistent with our earlier experiments, a 30 min ketamine application to wild-type littermate control mice produced robust potentiation coupled with a significant increase in the slope of input–output curve without altering paired-pulse response ratios (Fig. 5*A–C*). In contrast, the same treatment failed to induce significant potentiation in slices prepared from constitutive eEF2 kinase knock-out mice (Fig. 5*D–F*). These results demonstrate that the absence of eEF2 kinase, a key biochemical transducer of resting NMDAR activity, eliminates the synaptic potentiation as well as the antidepressant response seen after ketamine treatment.

To investigate the mechanism underlying the increase in synaptic efficacy seen after ketamine administration, we focused our attention on alterations in surface expression levels of AMPARs. Biochemical measurements of surface-expressed AMPARs were assessed by surface biotinylation in eEF2 kinase knock-out mice and wild-type littermate control mice following low-dose ketamine administration (Fig. 6*A*,*B*). This analysis revealed that ketamine triggers an increase in surface levels of GluA1 and GluA2, which depends on eEF2 kinase (Fig. 6*C*,*D*). To test this result further, we examined whether the enhanced transmission seen after NMDAR block is sensitive to 1-napthylacetylspermine (NASPM), a specific antagonist of GluA2-lacking AMPARs (Sutton et al., 2006). NASPM application did not inhibit the effect of MK801 or ketamine on synaptic strength, which is consistent with coregulation of GluA1 and GluA2 subunits (Fig. 7*A*,*B*). In contrast, perfusion of DNQX, a specific blocker of AMPARs regardless of subunit composition, at a low dose (2 μM) reduced the potentiated response seen after application of ketamine (Fig. 7*C*) or MK-801 (Fig. 7*D*). In agreement with this premise, application of ketamine to hippocampal slices from GluA2 knock-out mice (Jia et al., 1996) did not elicit a significant change in synaptic strength (Fig. 7*E*,*F*). In contrast, slices from wild-type littermates showed significant change in synaptic strength after treatment with ketamine (Fig. 7*E*,*F*). Moreover, the acute antidepressant-like effects of ketamine, as assessed by forced swim test (Fig. 8*A*) or the novelty-suppressed feeding paradigm (Fig. 8*B*,*C*), were not present in GluA2 knock-out mice. Together with earlier be-

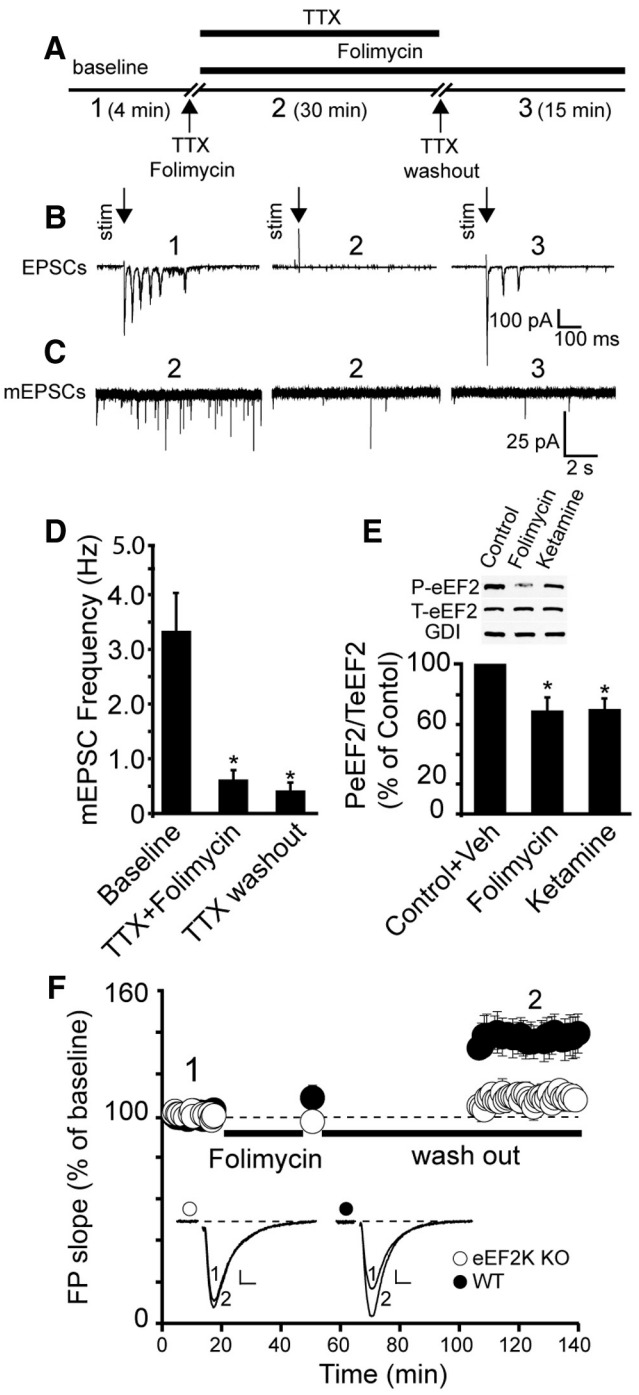

Figure 9. Selective suppression of spontaneous release via application of folimycin at rest is sufficient to elicit eEF2 kinase-dependent synaptic potentiation. ***A***, Experimental design for whole-cell recordings in the presence of folimycin. ***B***, ***C***, Representative traces of evoked (***B***) and spontaneous (***C***) postsynaptic currents during different stages of the experiment (1, 2, 3). ***B***, Recording evoked neuronal activity in dissociated hippocampal cultures for 4 min in Tyrode's solution (1), in presence of 10 μM TTX and 80 nM folimycin for 30 min (2), and after TTX washout (3). ***C***, Recording spontaneous neuronal activity (mEPSC) in dissociated hippocampal cultures 10 min after application of TTX and folimycin (2), 30 min after application of TTX and folimycin (2), and after TTX washout (3). ***D***, mEPSC frequency is significantly reduced in the presence of folimycin with or without TTX ($n = 5$, $p < 0.001$; mean ± SEM). ***E***, Immunoblot analysis of phospho-eEF2 and total-eEF2 proteins in total protein lysates from dissociated hippocampal cultures indicates that the level of eEF2 phosphorylation in cultures treated with folimycin or ketamine is significantly decreased compared with control cultures treated with vehicle ($n = 5$, $p < 0.02$). Plotted are phospho-eEF2/total eEF2 ratios as percentage of control. ***F***, FPs were recorded in eEF2K knock-out (KO) mice and in wild-type (WT) littermate control mice. In WT slices (filled circles, $n = 5$), folimycin induced synaptic strength facilitation. In contrast, no changes were observed in slices from eEF2K KO mice after application of folimycin ($n = 9$). Plotted are FP initial slopes (mean ± SEM) as a function of time. Inset, Representative waveforms from WT and eEF2K KO slices, recorded at different time points (1, 2). One-way ANOVA with repeated measurements, $F_{(39,157)} = 2.85$, $p = 0.001$; with Holm-Sidak *post hoc* test, $p < 0.05$. Scale bar, 0.2 mV/5 ms.

havioral studies, these results further substantiate the role of AMPARs as downstream synaptic targets of ketamine's rapid antidepressant action (Maeng et al., 2008; Autry et al., 2011).

Selective suppression of spontaneous release via application of folimycin at rest is sufficient to elicit eEF2 kinase-dependent synaptic potentiation

Our data support a model in which NMDAR activity at rest, in the absence of action potential firing, helps maintain synaptic efficacy via activation of eEF2 kinase and suppression of protein translation. In turn, application of NMDAR blockers, such as ketamine, in the absence of activity inhibits this tonic suppression and results in robust potentiation of synaptic efficacy by increasing surface expression of GluA1 and GluA2 AMPAR subunits. These data point to a key role of NMDAR-mediated spontaneous neurotransmission in homeostatic maintenance of synaptic efficacy. Accordingly, our hypothesis is that inhibition of this resting level of neurotransmission leads to rapid augmentation of synaptic efficacy. To directly test this premise, we investigated whether selective presynaptic suppression of spontaneous neurotransmitter release mimics the action of NMDAR blockers.

To inhibit quantal spontaneous neurotransmitter release, we used the vacuolar ATPase blocker folimycin, which impairs synaptic vesicle reacidification and thus blocks neurotransmitter refilling after endocytosis (Zhou et al., 2000; Sara et al., 2005; Ertunc et al., 2007). The experimental design for this study was based on previous work demonstrating that folimycin treatment in the absence of stimulation leads to neurotransmitter depletion selectively from spontaneously recycling synaptic vesicles and inhibition of spontaneous neurotransmission (Sara et al., 2005; Ertunc et al., 2007; Povysheva and Johnson, 2012) but largely spares subsequent evoked release (Sara et al., 2005; Ertunc et al., 2007). However, evoked release can also be suppressed once stimulation is resumed in the presence of folimycin (Ertunc et al., 2007). Here, we validated these earlier findings by applying folimycin onto hippocampal neurons for 30 min in the presence of TTX to eliminate background activity (Fig. 9*A*,*B*). In this setting, folimycin application produced a substantial reduction in the frequency of mEPSCs (Fig. 9*C*,*D*). However, evoked synaptic currents could still be elicited after removal of TTX (Fig. 9*B*). This folimycin treatment also induced a significant reduction in eEF2 phosphorylation to a level comparable to the effect of ketamine (Fig. 9*E*), suggesting that selective manipulation of spontaneous neurotransmission has similar effects on signal transduction mediated through eEF2 kinase as blocking NMDARs at rest. We also found that 30 min perfusion of folimycin onto acute hippocampal slices in the absence of concurrent stimulation elicited robust synaptic potentiation mimicking the effect of ketamine or MK801 (Fig. 9*F*). Importantly, the same folimycin treatment failed to elicit significant potentiation in slices from eEF2 kinase knock-outs, providing further support for the involvement of this pathway in mediating synaptic efficacy. Results of the present study provide further support for the premise that NMDAR activity at rest is indeed triggered by spontaneous glutamate release leading to tonic activation of eEF2 kinase (Fig. 9*F*). In future

←

experiments, selectively targeting spontaneous neurotransmission *in vivo* will be necessary to further assess the potential of these mechanisms to trigger rapid antidepressant responses. Unfortunately, unlike ketamine, folimycin is not amenable to *in vivo* experiments that involve peripheral drug administration and robust brain penetration to test this premise *in vivo* on rapid antidepressant responses.

Discussion

In this study, we conducted electrophysiological, biochemical, and behavioral experiments to analyze the synaptic basis of the antidepressant-like behavioral effects triggered by acute ketamine application. We found that ketamine applied to hippocampal slices potentiates AMPAR-mediated evoked neurotransmission detected in the CA1 region within 30 min. This potentiation was not coupled to a change in paired-pulse facilitation, arguing against a potential role of increased presynaptic release probability in this process. These findings were not restricted to ketamine but were also detectable with MK-801, supporting a direct involvement of NMDAR blockade in subsequent synaptic potentiation. Moreover, when we tested the role of baseline activity via coapplication of ketamine and TTX to suppress Na^+ channel function, we found that ketamine-mediated synaptic potentiation could occur in the absence of action potential firing. This result provides a rather rigorous confirmation of the premise that suppression of spontaneous NMDAR-mediated mEPSCs is the major driver for this synaptic potentiation. This notion agrees with earlier findings where spontaneous mEPSCs were shown to possess a sizable NMDAR-mediated component in physiological levels of extracellular Mg^{2+} due to incomplete channel block (Espinosa and Kavalali, 2009; Povysheva and Johnson, 2012). These data demonstrate that the ketamine-mediated synaptic potentiation requires protein synthesis, as judged by its sensitivity to anisomycin, and is dependent on BDNF expression as ketamine application failed to elicit potentiation in slices from BDNF knock-out mice. Collectively, these results identify critical determinants of how blocking spontaneous neurotransmission impacts synaptic plasticity.

These electrophysiological observations are in line with our earlier behavioral analysis of ketamine's rapid antidepressant action (Autry et al., 2011), revealing striking parallels between the mechanism of this synaptic potentiation and the behavioral effect in terms of their dependence on protein translation and BDNF expression. Here, we extended the parallels between the synaptic and behavioral processes using eEF2 kinase knock-outs. Our data show that both the synaptic potentiation and the antidepressant effects triggered by ketamine are abolished in the absence of eEF2 kinase, suggesting that the eEF2 kinase-mediated protein translation regulation was rendered insensitive to NMDAR function in the eEF2 kinase knock-out.

Surface biotinylation experiments demonstrated that ketamine-mediated synaptic potentiation was coupled to an increase in surface expression of both GluA1 and GluA2 subunits of AMPARs. These biochemical observations could also be validated by experiments performed in GluA2 knock-out mice where ketamine-mediated synaptic potentiation and behavioral antidepressant effects were both absent. In agreement with a critical role of AMPARs in the ketamine-mediated potentiation as well as in ketamine's antidepressant responses (Autry et al., 2011), application of 2 μM DNQX could inhibit the increase in synaptic efficacy seen after ketamine application. Moreover, the specificity of these observations to AMPAR function was also supported by the relative conservation of NMDA-fEPSP input–output relationships after ketamine treatment. Together, these findings support a key role for a homeostatic increase in postsynaptic AMPARs in ketamine's antidepressant response (Kavalali and Monteggia, 2012) and argue against an increase in synapse formation as a factor contributing to the initial phases of ketamine's rapid antidepressant action (Duman and Aghajanian, 2012).

Finally, we took advantage of the previously characterized use-dependent effect of vacuolar ATPase blockers, such as folimycin, on neurotransmission (Sara et al., 2005; Ertunc et al., 2007) to selectively suppress spontaneous neurotransmitter release via application of the blocker at rest. This maneuver spared the subsequent evoked neurotransmission and, in addition, resulted in an eEF2 kinase-dependent synaptic potentiation similar to the postsynaptic effect of NMDAR blockers. This result establishes a key link between the resting presynaptic vesicle trafficking pathway that gives rise to spontaneous neurotransmitter release and the postsynaptic signaling mechanism mediated by NMDAR activity and eEF2 kinase function.

Collectively, these findings identify a critical role for quantal spontaneous glutamate release in the maintenance of synaptic efficacy via its tonic activation of eEF2 kinase. Conversely, a reduction in spontaneous glutamate release triggers a rapid increase in synaptic efficacy. This action of spontaneous glutamate release is independent of evoked neurotransmission, although it has a potent impact on the efficacy of evoked neurotransmission. Our behavioral experiments suggest that the same mechanisms can be exploited to trigger plasticity and induce behavioral effects, as seen in the rapid antidepressant action of ketamine. Together, these findings put forth the novel hypothesis that spontaneous neurotransmission may provide a viable target for therapeutic interventions against neuropsychiatric disorders.

References

Aoto J, Nam CI, Poon MM, Ting P, Chen L (2008) Synaptic signaling by all-trans retinoic acid in homeostatic synaptic plasticity. Neuron 60:308–320. CrossRef Medline

Atasoy D, Ertunc M, Moulder KL, Blackwell J, Chung C, Su J, Kavalali ET (2008) Spontaneous and evoked glutamate release activates two populations of NMDA receptors with limited overlap. J Neurosci 28:10151–10166. CrossRef Medline

Autry AE, Adachi M, Nosyreva E, Na ES, Los MF, Cheng PF, Kavalali ET, Monteggia LM (2011) NMDA receptor blockade at rest triggers rapid behavioural antidepressant responses. Nature 475:91–95. CrossRef Medline

Berman RM, Cappiello A, Anand A, Oren DA, Heninger GR, Charney DS, Krystal JH (2000) Antidepressant effects of ketamine in depressed patients. Biol Psychiatry 47:351–354. CrossRef Medline

Chung HJ, Xia J, Scannevin RH, Zhang X, Huganir RL (2000) Phosphorylation of the AMPA receptor subunit GluR2 differentially regulates its interaction with PDZ domain-containing proteins. J Neurosci 20:7258–7267. Medline

Duman RS, Aghajanian GK (2012) Synaptic dysfunction in depression: potential therapeutic targets. Science 338:68–72. CrossRef Medline

Ertunc M, Sara Y, Chung C, Atasoy D, Virmani T, Kavalali ET (2007) Fast synaptic vesicle reuse slows the rate of synaptic depression in the CA1 region of hippocampus. J Neurosci 27:341–354. CrossRef Medline

Espinosa F, Kavalali ET (2009) NMDA receptor activation by spontaneous glutamatergic neurotransmission. J Neurophysiol 101:2290–2296. Medline

Frank CA, Kennedy MJ, Goold CP, Marek KW, Davis GW (2006) Mechanisms underlying the rapid induction and sustained expression of synaptic homeostasis. Neuron 52:663–677. CrossRef Medline

Herman MA, Jahr CE (2007) Extracellular glutamate concentration in hippocampal slice. J Neurosci 27:9736–9741. CrossRef Medline

Heynen AJ, Yoon BJ, Liu CH, Chung HJ, Huganir RL, Bear MF (2003) Molecular mechanism for loss of visual cortical responsiveness following brief monocular deprivation. Nat Neurosci 6:854–862. Medline

Huber KM, Kayser MS, Bear MF (2000) Role for rapid dendritic protein

synthesis in hippocampal mGluR-dependent long-term depression. Science 288:1254–1257. CrossRef Medline

Jia Z, Agopyan N, Miu P, Xiong Z, Henderson J, Gerlai R, Taverna FA, Velumian A, MacDonald J, Carlen P, Abramow-Newerly W, Roder J (1996) Enhanced LTP in mice deficient in the AMPA receptor GluR2. Neuron 17:945–956. CrossRef Medline

Jin I, Puthanveettil S, Udo H, Karl K, Kandel ER, Hawkins RD (2012) Spontaneous transmitter release is critical for the induction of long-term and intermediate-term facilitation in *Aplysia*. Proc Natl Acad Sci U S A 109: 9131–9136. CrossRef Medline

Katz B (1969) The release of neural transmitter substances. Liverpool, UK: Liverpool UP.

Kavalali ET, Monteggia LM (2012) Synaptic mechanisms underlying rapid antidepressant action of ketamine. Am J Psychiatry 169:1150–1156. CrossRef Medline

Kavalali ET, Klingauf J, Tsien RW (1999) Activity-dependent regulation of synaptic clustering in a hippocampal culture system. Proc Natl Acad Sci U S A 96:12893–12900. CrossRef Medline

Kotermanski SE, Johnson JW (2009) Mg^{2+} imparts NMDA receptor subtype selectivity to the Alzheimer's drug memantine. J Neurosci 29:2774–2779. CrossRef Medline

Lee MC, Yasuda R, Ehlers MD (2010) Metaplasticity at single glutamatergic synapses. Neuron 66:859–870. CrossRef Medline

Lindskog M, Li L, Groth RD, Poburko D, Thiagarajan TC, Han X, Tsien RW (2010) Postsynaptic GluA1 enables acute retrograde enhancement of presynaptic function to coordinate adaptation to synaptic inactivity. Proc Natl Acad Sci U S A 107:21806–21811. CrossRef Medline

Maeng S, Zarate CA Jr, Du J, Schloesser RJ, McCammon J, Chen G, Manji HK (2008) Cellular mechanisms underlying the antidepressant effects of ketamine: role of alpha-amino-3-hydroxy-5-methylisoxazole-4-propionic acid receptors. Biol Psychiatry 63:349–352. CrossRef Medline

Monteggia LM, Barrot M, Powell CM, Berton O, Galanis V, Gemelli T, Meuth S, Nagy A, Greene RW, Nestler EJ (2004) Essential role of brain-derived neurotrophic factor in adult hippocampal function. Proc Natl Acad Sci U S A 101:10827–10832. CrossRef Medline

Park S, Park JM, Kim S, Kim JA, Shepherd JD, Smith-Hicks CL, Chowdhury S, Kaufmann W, Kuhl D, Ryazanov AG, Huganir RL, Linden DJ, Worley PF (2008) Elongation factor 2 and fragile X mental retardation protein control the dynamic translation of Arc/Arg3.1 essential for mGluR-LTD. Neuron 59:70–83. CrossRef Medline

Povysheva NV, Johnson JW (2012) Tonic NMDA receptor-mediated current in prefrontal cortical pyramidal cells and fast-spiking interneurons. J Neurophysiol 107:2232–2243. CrossRef Medline

Price RB, Nock MK, Charney DS, Mathew SJ (2009) Effects of intravenous ketamine on explicit and implicit measures of suicidality in treatment-resistant depression. Biol Psychiatry 66:522–526. CrossRef Medline

Ryazanov AG (2002) Elongation factor-2 kinase and its newly discovered relatives. FEBS Lett 514:26–29. CrossRef Medline

Sara Y, Virmani T, Deák F, Liu X, Kavalali ET (2005) An isolated pool of vesicles recycles at rest and drives spontaneous neurotransmission. Neuron 45:563–573. CrossRef Medline

Sutton MA, Ito HT, Cressy P, Kempf C, Woo JC, Schuman EM (2006) Miniature neurotransmission stabilizes synaptic function via tonic suppression of local dendritic protein synthesis. Cell 125:785–799. CrossRef Medline

Sutton MA, Taylor AM, Ito HT, Pham A, Schuman EM (2007) Postsynaptic decoding of neural activity: eEF2 as a biochemical sensor coupling miniature synaptic transmission to local protein synthesis. Neuron 55:648–661. CrossRef Medline

Zarate CA Jr, Singh JB, Carlson PJ, Brutsche NE, Ameli R, Luckenbaugh DA, Charney DS, Manji HK (2006) A randomized trial of an N-methyl-D-aspartate antagonist in treatment-resistant major depression. Arch Gen Psychiatry 63:856–864. CrossRef Medline

Zhou Q, Petersen CC, Nicoll RA (2000) Effects of reduced vesicular filling on synaptic transmission in rat hippocampal neurones. J Physiol 525: 195–206. Medline